

A generalized model of non-linear viscoelasticity: numerical issues and applications

M. de Buhan^{1,2,*},[†] and P. Frey^{1,2}

¹UPMC Univ Paris 06, UMR 7598, Laboratoire J.L. Lions, F-75005 Paris, France

²Universidad de Chile, FCFyM, Depto. de Ingeniería Matemática, Santiago, Chile

SUMMARY

In this paper, we consider a non-linear viscoelastic model with internal variable, thoroughly analyzed by Le Tallec *et al.* (*Comput. Methods Appl. Mech. Engrg* 1993; **109**:233–258). Our aim is to study here the implementation in three dimensions of a generalized version of this model. Computational results will be analyzed to validate our model on toy problems without geometric complexity, for which pseudo-analytical solutions are known. At the end, we present a three-dimensional numerical simulation on a mechanical device. Copyright © 2011 John Wiley & Sons, Ltd.

Received 29 April 2010; Revised 26 October 2010; Accepted 4 November 2010

KEY WORDS: non-linear viscoelasticity; finite element method; mesh adaptation

1. INTRODUCTION

In this paper, we address the numerical aspects of a non-linear viscoelastic problem. Among the various types of non-linear viscoelastic models available, we have deliberately considered the model that introduces an additional internal variable governed by a differential equation in time, initially presented by Simo [1] and Lubliner [2] and mathematically analyzed in [3, 4]. We describe here the discretization and the implementation in three dimensions using triangulations of a generalized version of this model, in a sense that will be made clear hereafter.

This paper is divided into three parts. In the first part, we develop the non-linear viscoelastic model. The second part describes the discretization stage and the numerical resolution of the mechanical model. The last part presents the validation of the resolution on a pseudo-analytical solution and a three-dimensional example on a mechanical device.

2. THE GENERALIZED MODEL

At first, we present the viscoelastic model in large strains that we used in numerical simulations and we explain how our version differs and generalizes the classical model [1].

Let Ω be a connected and bounded open set of \mathbb{R}^3 corresponding to the reference configuration (Figure 1). We suppose that the boundary Γ of Ω is Lipschitz-continuous; thus, the outer unit

*Correspondence to: M. de Buhan, UPMC Univ Paris 06, UMR 7598, Laboratoire J.L. Lions, F-75005 Paris, France.

[†]E-mail: debuhan@ann.jussieu.fr

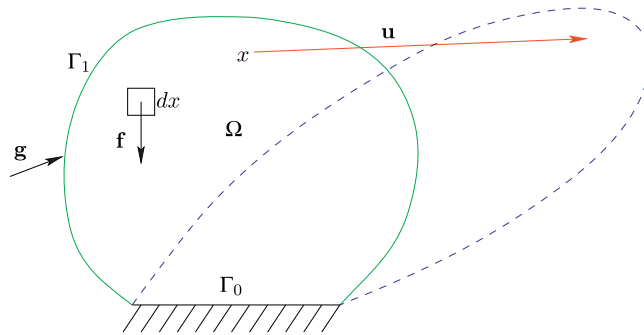


Figure 1. Deformation of the domain Ω .

normal vector n is well defined at each boundary point. We assume also that the boundary can be decomposed into $\Gamma = \bar{\Gamma}_0 \cup \bar{\Gamma}_1$ with $\Gamma_0 \cap \Gamma_1 = \emptyset$. The model problem we consider is the following:

Find the displacement vector \mathbf{u} solving:

$$\begin{aligned} -\nabla \cdot \mathbf{T} &= \mathbf{f} && \text{in } \Omega, \\ \mathbf{u} &= \mathbf{u}_0 && \text{on } \Gamma_0, \\ \mathbf{T} \cdot \mathbf{n} &= \mathbf{g} && \text{on } \Gamma_1. \end{aligned}$$

Here, \mathbf{f} (resp. \mathbf{g}) represents the body (resp. surface) forces, expressed in the reference configuration. The constitutive law is then given by the following relation that relates the first Piola–Kirchhoff stress tensor[‡] \mathbf{T} to the gradient of deformation $\mathbf{F} = \mathbf{I} + \nabla \mathbf{u}$:

$$\mathbf{T} = \frac{dW}{d\mathbf{F}} - p\mathbf{F}^{-t}. \tag{1}$$

In the viscoelastic model we consider here, the internal energy W of the system can be written as follows:

$$W(\mathbf{C}, \mathbf{G}_1, \dots, \mathbf{G}_m) = W_0(\mathbf{C}) + \sum_{i=1}^m W_i(\mathbf{C}; \mathbf{G}_i), \quad m \in \mathbb{N}^*, \tag{2}$$

where the right Cauchy–Green tensor \mathbf{C} is defined as:

$$\mathbf{C} = \mathbf{F}^t \mathbf{F} = \mathbf{I} + \nabla \mathbf{u} + \nabla \mathbf{u}^t + \nabla \mathbf{u} \cdot \nabla \mathbf{u}^t,$$

and where the tensors \mathbf{G}_i , for $i \in \llbracket 1, m \rrbracket$, are a finite number of internal variables used to measure the deformation of dashpots embedded in the material. The evolution of these internal variables is described by the set of following equations:

$$\begin{aligned} v_i \dot{\mathbf{G}}_i^{-1} &= \frac{\partial W}{\partial \mathbf{G}_i} + q_i \mathbf{G}_i^{-1} && \text{in } \Omega \quad \forall i \in \llbracket 1, m \rrbracket, \\ \mathbf{G}_i(0) &= \mathbf{I} && \text{in } \Omega \end{aligned} \tag{3}$$

with v_i , for $i \in \llbracket 1, m \rrbracket$, the viscosity coefficients. The pressures p and q_i , for $i \in \llbracket 1, m \rrbracket$, occurring in Equations (1) and (3) are the Lagrange multipliers associated with the incompressibility constraints:

$$\det(\mathbf{F}) = \det(\mathbf{G}_i) = 1 \quad \forall i \in \llbracket 1, m \rrbracket.$$

[‡]Using the classical notation introduced by Ciarlet [5].

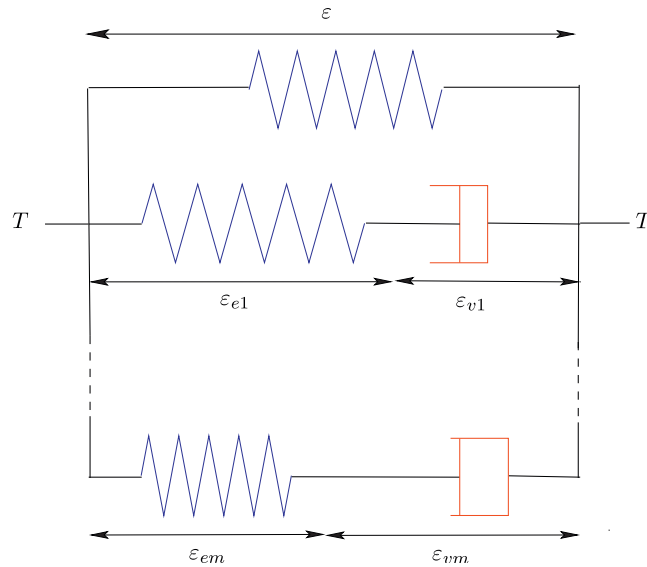


Figure 2. Generalized Maxwell model. $\boldsymbol{\varepsilon}$, $\boldsymbol{\varepsilon}_{ei}$, $\boldsymbol{\varepsilon}_{vi}$ for $i \in \llbracket 1, m \rrbracket$, are the total, elastic and viscoelastic linearized stress tensors.

At this point, we observe that this model is slightly different from the model described in [3], in the sense that it contains supplementary internal variables, hereby justifying its denomination of generalized model. In other words, if the model of [3] is a non-linear version of the Maxwell model, by analogy our model can be seen as a non-linear version of the generalized Maxwell model (see Figure 2). In its spirit, this model is close to the model described in [6], initially proposed in another context for dealing with ligaments. Its main strength relies on its versatility for handling complex behaviors (e.g. to account for various dissipation time) that could not be captured with the classical models. This rather complex formulation is indeed required by the application we have in mind, as will be emphasized in the numerical examples presented in Section 4.2.

In view of its numerical resolution using the finite element method, a weak formulation of this problem shall be first written, which leads now to solve:

Find $\mathbf{u} - \mathbf{u}_0 \in \mathcal{V}$, $p \in \mathcal{P}$, $\mathbf{G}_i \in \mathcal{H}$ and $q_i \in \mathcal{Q}$, for $\forall i \in \llbracket 1, m \rrbracket$, such that:

$$\begin{aligned} \int_{\Omega} \left(2\mathbf{F} \frac{\partial W}{\partial \mathbf{C}}(\mathbf{C}, \mathbf{G}_1, \dots, \mathbf{G}_m) - p \mathbf{F}^{-t} \right) : \nabla \mathbf{v} \, dx &= \int_{\Omega} \mathbf{f} \cdot \mathbf{v} \, dx + \int_{\Gamma_1} \mathbf{g} \cdot \mathbf{v} \, d\gamma \quad \forall \mathbf{v} \in \mathcal{V}, \\ \int_{\Omega} \hat{p} (\det(\mathbf{F}) - 1) \, dx &= 0 \quad \forall \hat{p} \in \mathcal{P}, \\ \int_{\Omega} \left(-\frac{\partial W_i}{\partial y}(\mathbf{C} : \mathbf{G}_i) \mathbf{C} + v_i \dot{\mathbf{G}}_i^{-1} - q_i \mathbf{G}_i^{-1} \right) : \mathbf{H} \, dx &= 0 \quad \forall \mathbf{H} \in \mathcal{H}, \\ \int_{\Omega} \hat{q} (\det(\mathbf{G}_i) - 1) \, dx &= 0 \quad \forall \hat{q} \in \mathcal{Q}. \end{aligned} \tag{4}$$

The functional spaces \mathcal{V} , \mathcal{P} , \mathcal{H} and \mathcal{Q} are chosen accordingly, i.e. such that all integrals are well defined, and: $:$ denotes the double contraction of tensors. Furthermore, the energy function defined in (2) leads to write:

$$\frac{\partial W}{\partial \mathbf{C}}(\mathbf{C}, \mathbf{G}_1, \dots, \mathbf{G}_m) = \frac{\partial W_0}{\partial \mathbf{C}}(\mathbf{C}) + \sum_{i=1}^m \frac{\partial W_i}{\partial y}(\mathbf{C} : \mathbf{G}_i) \mathbf{G}_i.$$

Thus, the problem associates a non-linear PDE endowed with incompressibility conditions and m ODEs describing the time evolution of the internal variables.

3. NUMERICAL APPROXIMATION

In this part, following the outline of the paper [3], we explain the main stages of the discretization of our model and the resolution techniques that have been effectively implemented in this study. The spatial discretization involves $\mathbb{P}_0/\mathbb{P}_2$ Lagrange finite elements and the time discretization is based on an implicit Euler scheme. The linearized version of the resulting system derives naturally from a Newton method and is solved using an Augmented Lagrangian technique.

3.1. Space discretization

Hereafter, we consider a conforming triangulation \mathcal{T}_h of the computational domain Ω where h represents the characteristic mesh size. The variational approximation of the initial problem (4) is classically obtained by replacing the functional spaces \mathcal{V} , \mathcal{P} , \mathcal{H} and \mathcal{Q} by finite-dimensional subspaces \mathcal{V}_h , \mathcal{P}_h , \mathcal{H}_h and \mathcal{Q}_h , respectively. We are well aware that the choice of these spaces is of importance to ensure the stability of the resolution. An analysis stage must confirm the validity of this choice, although it is out of the scope of this paper. Namely, we have retained the following finite elements spaces:

$$\mathcal{V}_h = \{\mathbf{v}_h : \bar{\Omega} \rightarrow \mathbb{R}^3, \forall K \in \mathcal{T}_h, \mathbf{v}_h|_K \in \mathbb{P}_2^3, \mathbf{v}_h = \mathbf{0} \text{ on } \Gamma_0\},$$

$$\mathcal{P}_h = \mathcal{Q}_h = \{p_h : \bar{\Omega} \rightarrow \mathbb{R}, \forall K \in \mathcal{T}_h, p_h|_K \in \mathbb{P}_0\},$$

$$\mathcal{H}_h = \{\mathbf{H}_h : \bar{\Omega} \rightarrow \mathcal{U}, \forall K \in \mathcal{T}_h, \mathbf{H}_h|_K \in \mathbb{P}_0^5\},$$

where $\mathcal{U} = \{\mathbf{H} \in (\mathcal{M}_3)_{sym}, \det(\mathbf{H}) = 1\}$. Consequently, the problem (4) becomes:

Find $\mathbf{u}_h - \mathbf{u}_{0h} \in \mathcal{V}_h$, $p_h \in \mathcal{P}_h$, $\mathbf{G}_{ih} \in \mathcal{H}_h$ and $q_{ih} \in \mathcal{Q}_h$, for $i \in \llbracket 1, m \rrbracket$, such that:

$$\int_{\Omega} \left(2\mathbf{F}_h \frac{\partial W}{\partial \mathbf{C}}(\mathbf{C}_h, \mathbf{G}_{1h}, \dots, \mathbf{G}_{mh}) - p_h \mathbf{F}_h^{-t} \right) : \nabla \mathbf{v}_h \, dx = \int_{\Omega} \mathbf{f} \cdot \mathbf{v}_h \, dx + \int_{\Gamma_1} \mathbf{g} \cdot \mathbf{v}_h \, d\gamma \quad \forall \mathbf{v}_h \in \mathcal{V}_h,$$

$$\int_{\Omega} \hat{p}_h (\det(\mathbf{F}_h) - 1) \, dx = 0 \quad \forall \hat{p}_h \in \mathcal{P}_h,$$

$$\int_{\Omega} \left(-\frac{\partial W_i}{\partial y}(\mathbf{C}_h : \mathbf{G}_{ih}) \mathbf{C}_h + v_i \dot{\mathbf{G}}_{ih}^{-1} - q_{ih} \mathbf{G}_{ih}^{-1} \right) : \mathbf{H}_h \, dx = 0 \quad \forall \mathbf{H}_h \in \mathcal{H}_h,$$

$$\int_{\Omega} \hat{q}_h (\det(\mathbf{G}_{ih}) - 1) \, dx = 0 \quad \forall \hat{q}_h \in \mathcal{Q}_h.$$

As \mathcal{H}_h and \mathcal{Q}_h are spaces composed of piecewise constant functions, the last equations can be further simplified as:

$$-\frac{\partial W_i}{\partial y}(\mathbf{C}_h : \mathbf{G}_{ih}) \mathbf{C}_h + v_i \dot{\mathbf{G}}_{ih}^{-1} - q_{ih} \mathbf{G}_{ih}^{-1} = \mathbf{0} \quad \text{in each } K \in \mathcal{T}_h \quad \forall i \in \llbracket 1, m \rrbracket$$

$$\det(\mathbf{G}_{ih}) = 1 \quad \text{in each } K \in \mathcal{T}_h.$$

3.2. Time discretization

We focus now on the time discretization of the problem using an implicit Euler scheme, which is unconditionally stable. This is an essential requisite for dealing with the various time scales

occurring in viscoelastic phenomena. Let Δt be the time discretization step. The numerical scheme we considered leads to solve the following sequence of problems:

For $n \in \mathbb{N}$, find $\mathbf{u}_h^{n+1} - \mathbf{u}_{0h} \in \mathcal{V}_h$, $p_h^{n+1} \in \mathcal{P}_h$, $\mathbf{G}_{ih}^{n+1} \in \mathcal{H}_h$ and $q_{ih}^{n+1} \in \mathcal{Q}_h$, for $i \in \llbracket 1, m \rrbracket$, solving:

$$\int_{\Omega} \left(2\mathbf{F}_h^{n+1} \frac{\partial W}{\partial \mathbf{C}}(\mathbf{C}_h^{n+1}, \mathbf{G}_{1h}^{n+1}, \dots, \mathbf{G}_{mh}^{n+1}) - p_h^{n+1} (\mathbf{F}_h^{n+1})^{-t} \right) : \nabla \mathbf{v}_h \, dx = \int_{\Omega} \mathbf{f} \cdot \mathbf{v}_h \, dx + \int_{\Gamma_1} \mathbf{g} \cdot \mathbf{v}_h \, d\gamma \quad \forall \mathbf{v}_h \in \mathcal{V}_h,$$

$$\int_{\Omega} \hat{p}_h (\det(\mathbf{F}_h^{n+1}) - 1) \, dx = 0 \quad \forall \hat{p}_h \in \mathcal{P}_h,$$

$$v_i \frac{(\mathbf{G}_{ih}^{n+1})^{-1} - (\mathbf{G}_{ih}^n)^{-1}}{\Delta t} - \frac{\partial W_i}{\partial \mathbf{y}}(\mathbf{C}_h^{n+1} : \mathbf{G}_{ih}^{n+1}) \mathbf{C}_h^{n+1} - q_{ih}^{n+1} (\mathbf{G}_{ih}^{n+1})^{-1} = \mathbf{0}, \quad \text{in each } K \in \mathcal{T}_h,$$

$$\det(\mathbf{G}_{ih}^{n+1}) = 1, \quad \text{in each } K \in \mathcal{T}_h,$$

endowed with the initial condition $\mathbf{G}_{ih}^0 = \mathbf{I}$, for $i \in \llbracket 1, m \rrbracket$.

The numerical resolution of this tedious problem is carried out in two steps. At first, we solve the evolution equations of the internal variables and express the latter in terms of the unknown \mathbf{C}_h^{n+1} . As the resulting problem depends only on \mathbf{C}_h^{n+1} , it can then be solved as a classical non-linear elastic problem.

3.3. Calculation of the viscoelastic variables

At each time step, we can compute each one of the m viscoelastic variables \mathbf{G}_{ih}^{n+1} , for $i \in \llbracket 1, m \rrbracket$, independently, all contributing to the physical dissipation phenomenon. This can be achieved solving the evolution equations in each element K in \mathcal{T}_h . To this end, we observe first that the problem can be rewritten, for each time step $n \in \mathbb{N}$, as the following minimization problem:

$$\mathbf{G}_{ih}^{n+1} = \arg \min_{\mathbf{H} \in \mathcal{U}} \left(W_i(\mathbf{C}_h^{n+1} : \mathbf{H}) + \frac{v_i}{\Delta t} (\mathbf{G}_{ih}^n)^{-1} : \mathbf{H} \right) \quad \forall i \in \llbracket 1, m \rrbracket.$$

Then, we consider \mathbf{G}_i as a function defined on \mathbb{R}^5 with value in \mathcal{U} of the form:

$$\begin{aligned} \mathbf{G}_i(\mathbf{Z}) &= Z_1(\mathbf{e}_1 \otimes \mathbf{e}_1) + Z_4(\mathbf{e}_2 \otimes \mathbf{e}_2) + Z_2(\mathbf{e}_1 \otimes \mathbf{e}_2 + \mathbf{e}_2 \otimes \mathbf{e}_1) + Z_3(\mathbf{e}_1 \otimes \mathbf{e}_3 + \mathbf{e}_3 \otimes \mathbf{e}_1) \\ &+ Z_5(\mathbf{e}_2 \otimes \mathbf{e}_3 + \mathbf{e}_3 \otimes \mathbf{e}_2) + \frac{1 + Z_1 Z_5^2 + Z_4 Z_3^2 - 2Z_2 Z_3 Z_5}{Z_1 Z_4 - Z_2^2} (\mathbf{e}_3 \otimes \mathbf{e}_3), \end{aligned}$$

where \otimes denotes the tensor product and we defined $\mathbf{Y}_i \in \mathbb{R}^5$ such that $\mathbf{G}_i(\mathbf{Y}_i) = \mathbf{G}_{ih}^{n+1}$, for $i \in \llbracket 1, m \rrbracket$. Thus, the minimization problem reads now:

$$\mathbf{Y}_i = \arg \min_{\mathbf{Z} \in \mathbb{R}^5} \left(W_i(\mathbf{C}_h^{n+1} : \mathbf{G}_i(\mathbf{Z})) + \frac{v_i}{\Delta t} (\mathbf{G}_{ih}^n)^{-1} : \mathbf{G}_i(\mathbf{Z}) \right),$$

that is also equivalent to solving:

$$\mathcal{F}_i(\mathbf{Y}_i, \mathbf{C}_h^{n+1}) = 0 \quad \forall i \in \llbracket 1, m \rrbracket, \tag{5}$$

where the function \mathcal{F}_i is defined, for all $(\mathbf{Z}, \mathbf{C}) \in \mathbb{R}^5 \times \mathcal{U}$ by:

$$\mathcal{F}_i(\mathbf{Z}, \mathbf{C}) = \left(\frac{\partial W_i}{\partial \mathbf{y}}(\mathbf{C} : \mathbf{G}_i(\mathbf{Z})) \mathbf{C} + \frac{v_i}{\Delta t} (\mathbf{G}_{ih}^n)^{-1} \right) : \frac{\partial \mathbf{G}_i}{\partial \mathbf{Z}}(\mathbf{Z}).$$

Next, we observe that the non-linear equation (5) defines an implicit function $\mathbf{Y}_i = \mathcal{Y}_i(\mathbf{C}_h^{n+1})$, for $i \in \llbracket 1, m \rrbracket$, that can be easily computed using a classical Newton method on \mathbb{R}^5 . At each iteration, the linear operator that needs to be inverted is given by:

$$\mathbf{K}_i = \frac{\partial \mathcal{F}_i}{\partial \mathbf{Z}}(\mathbf{Z}, \mathbf{C}) = \frac{\partial^2 W_i}{\partial y^2}(\mathbf{C} : \mathbf{G}_i(\mathbf{Z})) \left(\mathbf{C} : \frac{\partial \mathbf{G}_i}{\partial \mathbf{Z}}(\mathbf{Z}) \right) \otimes \left(\mathbf{C} : \frac{\partial \mathbf{G}_i}{\partial \mathbf{Z}}(\mathbf{Z}) \right) + \left(\frac{\partial W_i}{\partial y}(\mathbf{C} : \mathbf{G}_i(\mathbf{Z})) \mathbf{C} + \frac{v_i}{\Delta t} (\mathbf{G}_{ih}^n)^{-1} \right) : \frac{\partial^2 \mathbf{G}_i}{\partial \mathbf{Z}^2}(\mathbf{Z}).$$

3.4. Resolution of the elastic problem

According to the relation $\mathbf{G}_{ih}^{n+1} = \mathbf{G}_i(\mathcal{Y}_i(\mathbf{C}_h^{n+1})) = \mathcal{G}_i(\mathbf{C}_h^{n+1})$, for $i \in \llbracket 1, m \rrbracket$, we can replace the viscoelastic variables in the original problem (4) that become now:

Find $\mathbf{u}_h^{n+1} - \mathbf{u}_{0h} \in \mathcal{V}_h$ and $p_h^{n+1} \in \mathcal{P}_h$ solving:

$$\int_{\Omega} \left(2\mathbf{F}_h^{n+1} \frac{\partial W}{\partial \mathbf{C}}(\mathbf{C}_h^{n+1}, \mathcal{G}_1(\mathbf{C}_h^{n+1}), \dots, \mathcal{G}_m(\mathbf{C}_h^{n+1})) - p_h^{n+1} (\mathbf{F}_h^{n+1})^{-t} \right) : \nabla \mathbf{v}_h \, dx = \int_{\Omega} \mathbf{f} \cdot \mathbf{v}_h \, dx + \int_{\Gamma_1} \mathbf{g} \cdot \mathbf{v}_h \, d\gamma \quad \forall \mathbf{v}_h \in \mathcal{V}_h,$$

$$\int_{\Omega} \hat{p}_h (\det(\mathbf{F}_h^{n+1}) - 1) \, dx = 0 \quad \forall \hat{p}_h \in \mathcal{P}_h.$$

Let $(\phi_j)_{j=1..N}$ be a basis of \mathcal{V}_h and $(\psi_j)_{j=1..M}$ be a basis of \mathcal{P}_h , respectively. If we consider the vector \mathbf{U}_h^{n+1} (resp. \mathbf{P}_h^{n+1}) of the components of $\mathbf{u}_h^{n+1} - \mathbf{u}_{0h}$ (resp. p_h^{n+1}) in the basis $(\phi_j)_{j=1..N}$ (resp. $(\psi_j)_{j=1..M}$), our finite element problem takes, at each time step n , the form of an algebraic system of $N + M$ non-linear equations with $N + M$ unknowns:

Find $(\mathbf{U}_h^{n+1}, \mathbf{P}_h^{n+1}) \in \mathbb{R}^N \times \mathbb{R}^M$ such that:

$$\mathcal{L}(\mathbf{U}_h^{n+1}, \mathbf{P}_h^{n+1}) = 0 \quad \text{in } \mathbb{R}^N \times \mathbb{R}^M,$$

with the notations, for all $(\mathbf{U}, \mathbf{P}) \in \mathbb{R}^N \times \mathbb{R}^M$:

$$\mathcal{L}_j(\mathbf{U}, \mathbf{P}) = \int_{\Omega} 2\mathbf{F} \frac{\partial W}{\partial \mathbf{C}}(\mathbf{C}, \mathcal{G}_1(\mathbf{C}), \dots, \mathcal{G}_m(\mathbf{C})) : \nabla \phi_j \, dx - \int_{\Omega} p \mathbf{F}^{-t} : \nabla \phi_j \, dx - \int_{\Omega} \mathbf{f} \cdot \phi_j \, dx - \int_{\Gamma_1} \mathbf{g} \cdot \phi_j \, d\gamma \quad \forall j \in \llbracket 1, N \rrbracket,$$

$$\mathcal{L}_{j+N}(\mathbf{U}, \mathbf{P}) = - \int_{\Omega} \psi_j (\det(\mathbf{F}) - 1) \, dx \quad \forall j \in \llbracket 1, M \rrbracket.$$

This system can be very large but sparse. It can be easily linearized by a Newton algorithm.

3.5. Linearization by a Newton method

To solve the non-linear equation $\mathcal{L}(\mathbf{U}_h^{n+1}, \mathbf{P}_h^{n+1}) = \mathbf{0}$ using Newton's method, we have to compute the gradient matrix $D\mathcal{L}/D(\mathbf{U}, \mathbf{P})$ that is defined for all $(\mathbf{U}, \mathbf{P}, \mathbf{V}, \mathbf{Q}) \in \mathbb{R}^N \times \mathbb{R}^M \times \mathbb{R}^N \times \mathbb{R}^M$ by:

$$\frac{\partial \mathcal{L}_j}{\partial \mathbf{U}}(\mathbf{U}, \mathbf{P}) \mathbf{V} = \int_{\Omega} \left(4 \frac{d}{d\mathbf{C}} \left(\frac{\partial W}{\partial \mathbf{C}}(\mathbf{C}, \mathcal{G}_1(\mathbf{C}), \dots, \mathcal{G}_m(\mathbf{C})) \right) : \mathbf{F}^t \nabla \mathbf{v} \right) : \mathbf{F}^t \nabla \phi_j \, dx + \int_{\Omega} 2 \frac{\partial W}{\partial \mathbf{C}}(\mathbf{C}, \mathcal{G}_1(\mathbf{C}), \dots, \mathcal{G}_m(\mathbf{C})) : \nabla \mathbf{v}^t \nabla \phi_j \, dx$$

$$\begin{aligned}
& - \int_{\Omega} p \left(\frac{\partial(\mathbf{F}^{-t})}{\partial \mathbf{F}} : \nabla \mathbf{v} \right) : \nabla \phi_j \, dx \quad \forall j \in \llbracket 1, N \rrbracket, \\
\frac{\partial \mathcal{L}_{j+N}}{\partial \mathbf{U}}(\mathbf{U}, \mathbf{P}) \mathbf{V} &= - \int_{\Omega} \psi_j \mathbf{F}^{-t} : \nabla \mathbf{v} \, dx \quad \forall j \in \llbracket 1, M \rrbracket, \\
\frac{\partial \mathcal{L}_j}{\partial \mathbf{P}}(\mathbf{U}, \mathbf{P}) \mathbf{Q} &= - \int_{\Omega} q \mathbf{F}^{-t} : \nabla \phi_j \, dx \quad \forall j \in \llbracket 1, N \rrbracket, \\
\frac{\partial \mathcal{L}_{j+N}}{\partial \mathbf{P}}(\mathbf{U}, \mathbf{P}) \mathbf{Q} &= 0, \quad \forall j \in \llbracket 1, M \rrbracket.
\end{aligned}$$

We notice that the differential

$$\frac{d}{d\mathbf{C}} \left(\frac{\partial W}{\partial \mathbf{C}}(\mathbf{C}, \mathcal{G}_1(\mathbf{C}), \dots, \mathcal{G}_m(\mathbf{C})) \right)$$

must be computed, which implies knowing the derivatives $\partial \mathcal{G}_i / \partial \mathbf{C}$, for $i \in \llbracket 1, m \rrbracket$. The implicit function theorem states that:

$$\begin{aligned}
\mathcal{F}_i(\mathbf{Y}_i, \mathbf{C}_h^{n+1}) = \mathbf{0} &\iff \mathbf{Y}_i = \mathcal{Y}_i(\mathbf{C}_h^{n+1}) \quad \text{and} \\
\frac{\partial \mathcal{Y}_i}{\partial \mathbf{C}}(\mathbf{C}_h^{n+1}) &= - \left(\frac{\partial \mathcal{F}_i}{\partial \mathbf{Z}}(\mathcal{Y}_i(\mathbf{C}_h^{n+1}), \mathbf{C}_h^{n+1}) \right)^{-1} \cdot \left(\frac{\partial \mathcal{F}_i}{\partial \mathbf{C}}(\mathcal{Y}_i(\mathbf{C}_h^{n+1}), \mathbf{C}_h^{n+1}) \right)^t,
\end{aligned}$$

and allows us to find the differential as follows:

$$\begin{aligned}
\frac{d}{d\mathbf{C}} \left(\frac{\partial W}{\partial \mathbf{C}}(\mathbf{C}, \mathcal{G}_1(\mathbf{C}), \dots, \mathcal{G}_m(\mathbf{C})) \right) &= \frac{\partial^2 W_0}{\partial \mathbf{C}^2}(\mathbf{C}) - \sum_{i=1}^m \mathbf{B}_i \cdot \mathbf{K}_i^{-1} \cdot \mathbf{B}_i^t \\
&\quad + \sum_{i=1}^m \frac{\partial^2 W_i}{\partial y^2}(\mathcal{G}_i(\mathbf{C}) : \mathbf{C})(\mathcal{G}_i(\mathbf{C}) \otimes \mathcal{G}_i(\mathbf{C})),
\end{aligned}$$

with, for $i \in \llbracket 1, m \rrbracket$:

$$\begin{aligned}
\mathbf{B}_i &= \frac{\partial \mathcal{F}_i}{\partial \mathbf{C}}(\mathcal{Y}_i(\mathbf{C}), \mathbf{C}) \\
&= \frac{\partial^2 W_i}{\partial y^2}(\mathbf{C} : \mathcal{G}_i(\mathbf{C})) \mathcal{G}_i(\mathbf{C}) \otimes \left(\mathbf{C} : \frac{\partial \mathbf{G}_i}{\partial \mathbf{Z}}(\mathcal{Y}_i(\mathbf{C})) \right) + \frac{\partial W_i}{\partial y}(\mathbf{C} : \mathcal{G}_i(\mathbf{C})) \frac{\partial \mathbf{G}_i}{\partial \mathbf{Z}}(\mathcal{Y}_i(\mathbf{C})).
\end{aligned}$$

Remark

It is well known that the Newton method is very sensitive to its initialization and may not converge in some cases, i.e. if the initial data differ largely from the solution. To overcome this drawback, the classical initialization strategy consists of using an incremental loading [7]. In this technique, the load acting on the body is applied as small increments. The equilibrium position is then computed at the end of each load increment using as initial guess the position obtained at the previous increment.

3.6. General algorithm

In this section, we summarize the main successive stages for solving the viscoelastic problem in large strains. Let us point out that the authors have implemented all data structures, finite elements libraries and non-linear system resolution techniques using C language (about 10 000 lines).

We initialize \mathbf{U} to the zero vector and \mathbf{P} to the hydrostatic pressure at rest. We set $\lambda = 0$ and we increase it iteratively by a small increment $\Delta \lambda$ until the value $\lambda = 1$ is attained. For each load

$(\lambda f, \lambda g)$, we compute the solution (\mathbf{U}, \mathbf{P}) by a Newton algorithm as follows:

- Initialization

We set $(\mathbf{U}_0, \mathbf{P}_0)$ equal to the solution at the previous loading step and we compute the residual:

$$\mathbf{R}_0 = \mathcal{L}(\mathbf{U}_0, \mathbf{P}_0).$$

- Iteration loop

Then, for each $k \geq 0$, knowing $\mathbf{U}_k, \mathbf{P}_k$ and \mathbf{R}_k , we obtain $\mathbf{U}_{k+1}, \mathbf{P}_{k+1}$ and \mathbf{R}_{k+1} by:

(a) computing the gradient matrix:

$$\mathbf{M}_k = \frac{D\mathcal{L}}{D(\mathbf{U}, \mathbf{P})}(\mathbf{U}_k, \mathbf{P}_k),$$

(b) solving the linear system:

$$\mathbf{M}_k(\Delta\mathbf{U}, \Delta\mathbf{P}) = -\mathbf{R}_k, \quad (6)$$

(c) updating the solution:

$$(\mathbf{U}_{k+1}, \mathbf{P}_{k+1}) = (\mathbf{U}_k, \mathbf{P}_k) + (\Delta\mathbf{U}, \Delta\mathbf{P}),$$

(d) solving the minimization problems on the viscoelastic variables using Newton loops to obtain $\mathcal{G}_i(\mathbf{C}_k), \forall i \in \llbracket 1, m \rrbracket$,

(e) evaluating the new residual:

$$\mathbf{R}_{k+1} = \mathcal{L}(\mathbf{U}_{k+1}, \mathbf{P}_{k+1}).$$

Remark

At each iteration of the Newton method, the linear system (6) can be solved by an augmented Lagrangian technique [8]. This iterative procedure consists of replacing at each iteration step the initial linear system by a simplest system that can be solved using a preconditioned conjugate gradient.

4. EXPERIMENTAL RESULTS

4.1. Validation

The aim of this section is to assess the numerical method by evaluating the discrepancy between the approximate solution and a pseudo-analytical solution, i.e. the exact solution in space approximated in time using a finite difference scheme. To this end, we considered the simplest case for which a pseudo-analytical solution can be computed, the compression of a cube fixed on one of its side. Indeed, in such a test case, there is no relevant geometric issue.

We describe hereafter the computation of this solution on the reference cube (Figure 3). Let H be the initial height of the sample and h its height after vertical compression (with respect to the Z -axis). We introduce the ratio:

$$\alpha = \frac{h}{H}.$$

Hence, we can define the transformation between the reference configuration (with respect to the variables X, Y, Z) and the deformed configuration (with respect to the variables x, y, z) by

$$x = \gamma X, \quad y = \gamma Y, \quad z = \alpha Z,$$

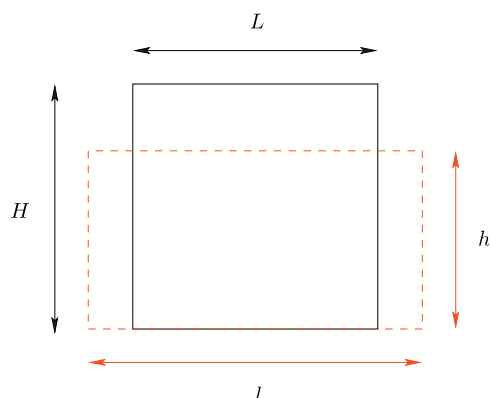


Figure 3. Compression of a cube: notations and characteristics variables.

where γ is the currently unknown horizontal dilatation coefficient, identical in X and Y , thanks to the symmetry of the problem. We can then compute the displacement vector \mathbf{u} , the gradient of deformation \mathbf{F} and the right Cauchy–Green tensor \mathbf{C} , respectively, as follows:

$$\mathbf{u} = \begin{pmatrix} (\gamma-1)X \\ (\gamma-1)Y \\ (\alpha-1)Z \end{pmatrix} \Rightarrow \mathbf{F} = \begin{pmatrix} \gamma & 0 & 0 \\ 0 & \gamma & 0 \\ 0 & 0 & \alpha \end{pmatrix} \Rightarrow \mathbf{C} = \begin{pmatrix} \gamma^2 & 0 & 0 \\ 0 & \gamma^2 & 0 \\ 0 & 0 & \alpha^2 \end{pmatrix},$$

and thanks to the incompressibility condition $\det(\mathbf{C})=1$, we can deduce

$$\gamma = \frac{1}{\sqrt{\alpha}},$$

yielding finally to:

$$\mathbf{C} = \begin{pmatrix} 1/\alpha & 0 & 0 \\ 0 & 1/\alpha & 0 \\ 0 & 0 & \alpha^2 \end{pmatrix}.$$

The energy function is chosen as a Moonley–Rivlin energy functional:

$$W_0(\mathbf{C}) = \mathcal{C}_{01}(I_1(\mathbf{C})-3) + \mathcal{C}_{02}(I_2(\mathbf{C})-3),$$

$$W_i(y) = \mathcal{C}_i(y-3) \quad \forall i \in \llbracket 1, m \rrbracket,$$

where $I_1(\mathbf{C}) = \text{tr}(\mathbf{C})$ and $I_2(\mathbf{C}) = \frac{1}{2}((\text{tr}(\mathbf{C}))^2 - \text{tr}(\mathbf{C}^2))$ are the first and second invariants of \mathbf{C} and \mathcal{C}_{01} , \mathcal{C}_{02} and \mathcal{C}_i , for $i \in \llbracket 1, m \rrbracket$, are constant coefficients in Pa. We need to compute the viscoelastic variables \mathbf{G}_i in view of evaluating the stress tensor \mathbf{T} . Each variable \mathbf{G}_i , for $i \in \llbracket 1, m \rrbracket$, satisfies the following ODE:

$$v_i \dot{\mathbf{G}}_i^{-1} - q_i \mathbf{G}_i^{-1} = \frac{\partial W_i}{\partial \mathbf{y}}(\mathbf{C}; \mathbf{G}_i) \mathbf{C} = \mathcal{C}_i \mathbf{C} \quad \forall i \in \llbracket 1, m \rrbracket,$$

with $\mathbf{G}_i(0) = \mathbf{I}$. This equation is discretized using the classical implicit finite differences scheme:

$$v_i \frac{(\mathbf{G}_i^{n+1})^{-1} - (\mathbf{G}_i^n)^{-1}}{\Delta t} - q_i^{n+1} (\mathbf{G}_i^{n+1})^{-1} = \mathcal{C}_i \mathbf{C}^{n+1},$$

thus leading to:

$$(\mathbf{G}_i^{n+1})^{-1} = \frac{\frac{v_i}{\Delta t}(\mathbf{G}_i^n)^{-1} + \mathcal{C}_i \mathbf{C}^{n+1}}{\frac{v}{\Delta t} - q_i^{n+1}} \quad \forall i \in \llbracket 1, m \rrbracket. \tag{7}$$

Here, the unknown variable q_i^{n+1} can be determined using the incompressibility condition $\det((\mathbf{G}_i^{n+1})^{-1}) = 1$, for $i \in \llbracket 1, m \rrbracket$, to obtain:

$$q_i^{n+1} = \frac{v_i}{\Delta t} - \left(\frac{v_i}{\Delta t}(\mathbf{G}_i^n)^{-1} + \frac{\mathcal{C}_i}{\alpha} \right)^{2/3} \left(\frac{v}{\Delta t}(\mathbf{G}_i^n)^{-1} + \mathcal{C}_i \alpha^2 \right)^{1/3},$$

which depends only on the time step n (since α is constant) and can be replaced in (7). At this stage, we can compute the stress tensor T using (1):

$$\begin{aligned} \mathbf{T} &= 2\mathbf{F} \frac{\partial W}{\partial \mathbf{C}}(\mathbf{C}, \mathbf{G}_1, \dots, \mathbf{G}_m) - p\mathbf{F}^{-t} \\ &= 2\mathbf{F} \left(\mathcal{C}_{01} + \mathcal{C}_{02}(\text{tr}(\mathbf{C})\mathbf{I} - \mathbf{C}) + \sum_{i=1}^m \mathcal{C}_i \mathbf{G}_i \right) - p\mathbf{F}^{-t}. \end{aligned}$$

Hence, the principal components of the diagonal tensor T can be expressed with respect to the elongation α as:

$$\begin{aligned} T_X = T_Y &= \frac{2}{\sqrt{\alpha}} \left(\mathcal{C}_{01} + \mathcal{C}_{02} \left(\alpha^2 + \frac{1}{\alpha} \right) + \sum_{i=1}^m \mathcal{C}_i (\mathbf{G}_i)_X \right) - \sqrt{\alpha} p, \\ T_Z &= 2\alpha \left(\mathcal{C}_{01} + \frac{2}{\alpha} \mathcal{C}_{02} + \sum_{i=1}^m \mathcal{C}_i (\mathbf{G}_i)_Z \right) - \frac{p}{\alpha}. \end{aligned}$$

By noticing that $T_X = T_Y = 0$, since the cube is not subjected to any load on its lateral sides, the pressure p can be determined as:

$$p = \frac{2}{\alpha} \left(\mathcal{C}_{01} + \mathcal{C}_{02} \left(\alpha^2 + \frac{1}{\alpha} \right) + \sum_{i=1}^m \mathcal{C}_i (\mathbf{G}_i)_X \right).$$

It remains then to compute the non-null vertical constraint T_Z as follows:

$$T_Z = 2(\alpha \mathcal{C}_{01} + \mathcal{C}_{02}) \left(1 - \frac{1}{\alpha^3} \right) + \sum_{i=1}^m 2\mathcal{C}_i \alpha \left((\mathbf{G}_i)_Z - \frac{1}{\alpha^3} (\mathbf{G}_i)_X \right).$$

As such, the pressure and the vertical constraint are both independent in space but need the computation of \mathbf{G}_i , for $i \in \llbracket 1, m \rrbracket$ to be estimated in time.

Now, we present the numerical result we obtained for this test case (for $\alpha=0.7$) (Figure 4). Table I reports the mechanical properties of our model. Figure 5 illustrates the time evolution of

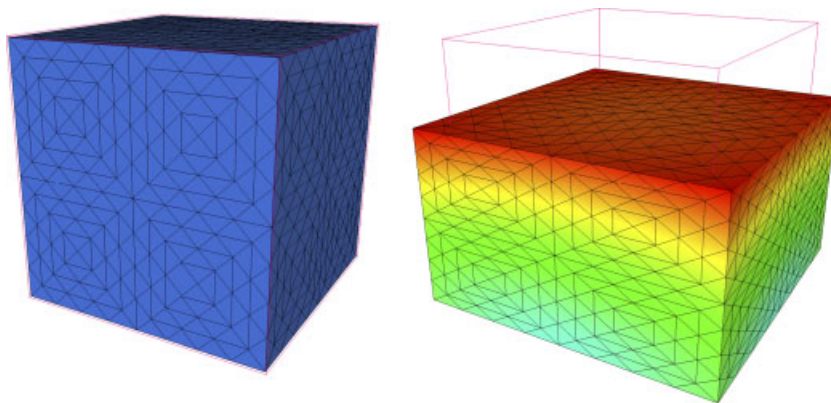


Figure 4. Configuration at rest (left), deformed configuration (right).

Table I. Mechanical properties used for the test case.

m	C_{01}	C_{10}	C_1	ν_1	C_2	ν_2
2	21	105	80	21500	150	115

the pressure, the vertical constraint and one internal variable corresponding to the numerical and the pseudo-analytical solutions.

Remark

In all examples, we have checked numerically (on the computational triangulation) that the total volume remains constant throughout the compression stage, in compliance with the incompressibility condition of the model.

4.2. Justification of the generalized formulation

Our objective is here to justify the choice of our generalized mechanical model and to show that it can fit an experimental data set much better than classical models. To this end, we compared the numerical results with experimental tests published in [9]. In this test, the geometry of the domain is considered non-relevant. The experiment corresponds to compressive tests on cylindrical samples (see Figure 6) at different strain rates.

In order to reproduce the experiments, we needed to extend the energy functional introduced in (2) as follows:

$$W_0(\mathbf{C}) = \mathcal{C}_{01}(I_1(\mathbf{C}) - 3) + \mathcal{C}_{02}(I_2(\mathbf{C}) - 3),$$

$$W_i(y) = \mathcal{C}_{i1}(y - 3) + \mathcal{C}_{i2}(y - 3)^2 \quad \forall i \in \llbracket 1, 2 \rrbracket.$$

Table II reports the coefficients used to carry out these tests.

Figure 7 shows the comparison between the experimental and the numerical solutions. We observe that both curves are well in accordance with each other. Notice that the stress–strain relation is non-linear and depends on the strain rate. Furthermore, it appears clearly that only an extended model is able to reproduce such complex behavior.

4.3. Example of a mechanical device

Figure 8 shows an example of a mechanical device corresponding to the domain $\Omega \subset 20 \times 20 \times 5$ cm, on which we applied a load $\mathbf{f} = (50, 50, 50) \text{ N m}^{-3}$, while maintaining fixed two branches on the (O, x, z) plane. The maximal deformation is about 10 cm, obtained using the values reported in Table I. The computational mesh contains 7402 vertices and 32 977 tetrahedra. The initial volume is $8.761 \times 10^2 \text{ cm}^3$ and the final volume after deformation is $8.760 \times 10^2 \text{ cm}^3$. In this example, we show the ability of dealing with the complex three-dimensional geometry of a mechanical device.

5. CONCLUSIONS AND PERSPECTIVES

This analysis has clearly shown the ability of our generalized model to deal with complex problems (both in terms of constitutive law and arbitrary geometry), essentially in structural mechanics. We could now envisage to address realistic problems for which experimental data are supplied and much be dealt with. This can be typically the case in biomechanical applications where flexible

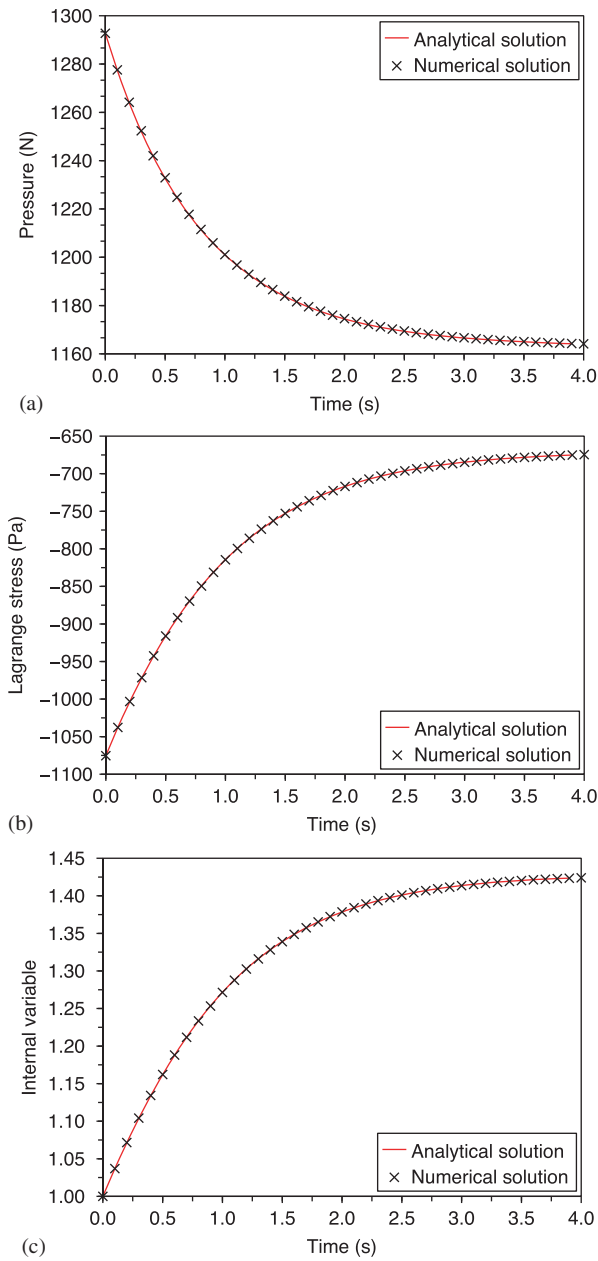


Figure 5. Evolution of (a) the pressure; (b) the vertical stress; and (c) the vertical component of the second internal variable with respect to time during the compression test. Comparison between the pseudo-analytical solution (continuous line) and the numerical solution (crosses).

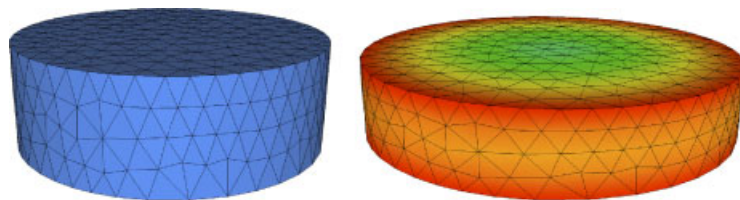


Figure 6. Configuration at rest (left). Deformed configuration (right).

Table II. Mechanical properties used for the first test case.

m	\mathcal{C}_{01}	\mathcal{C}_{10}	\mathcal{C}_{11}	\mathcal{C}_{12}	ν_1	\mathcal{C}_{21}	\mathcal{C}_{22}	ν_2
2	0	145	0	1300	35000	150	2000	200

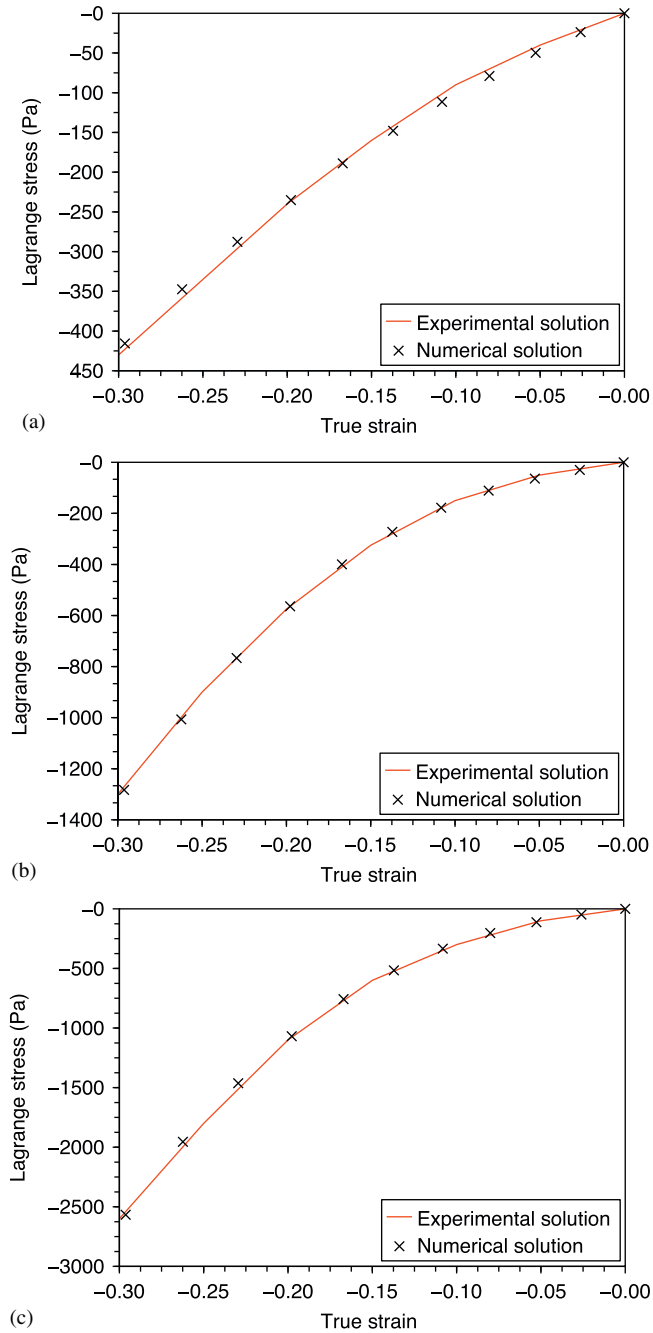


Figure 7. Relation between the Lagrange stress T and the true strain $\log(\alpha)$ for three compression rates: (a) $6.4 \times 10^{-6} \text{ s}^{-1}$; (b) $6.4 \times 10^{-3} \text{ s}^{-1}$; and (c) $6.4 \times 10^{-1} \text{ s}^{-1}$. Comparison between the experimental solutions reported by Miller [9] (lines) and the numerical solutions (crosses).

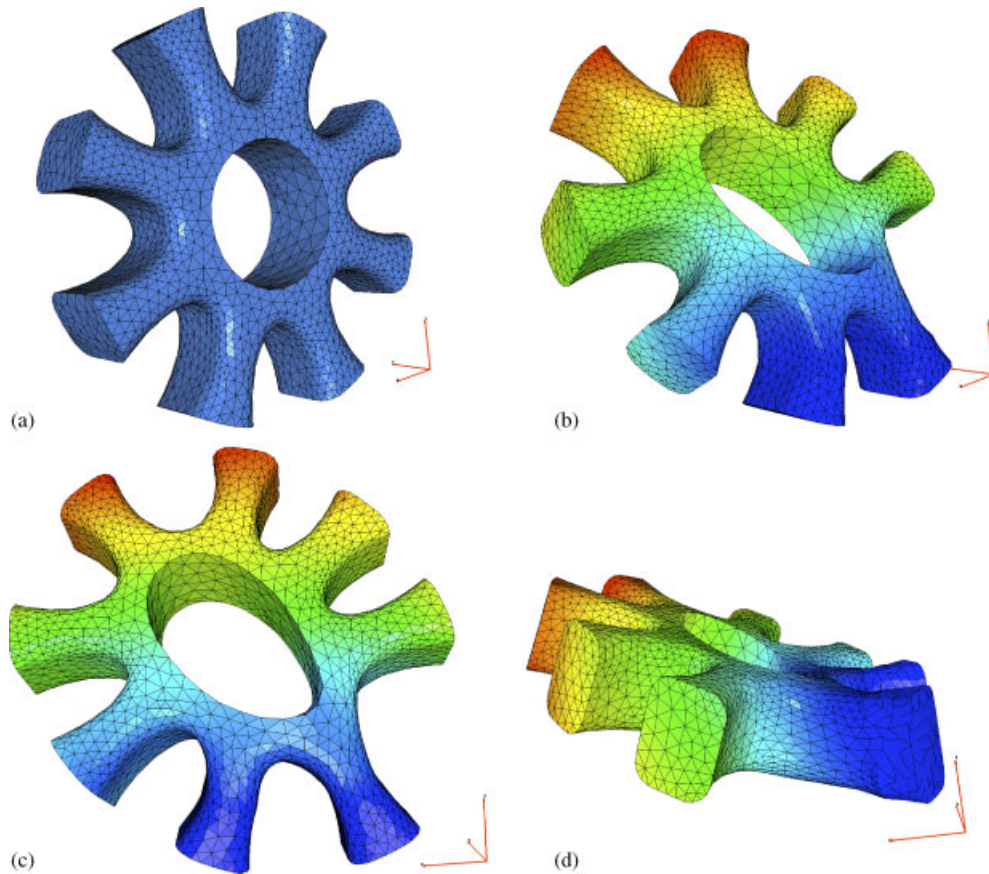


Figure 8. Computational mesh of the mechanical device (a). Deformation from various viewpoints (b),(c),(d).

models are favored because of the lack of modelling knowledge. On the other hand, this work can be considered as an essential (in terms of accuracy and efficiency) preliminary stage of a study on inverse problem whose purpose is to retrieve unknown coefficients.

ACKNOWLEDGEMENTS

This work has been supported by doctoral fellowships from CNRS and CONICYT.

REFERENCES

1. Simo JC. On a fully three-dimensional finite-strain viscoelastic damage model: formulation and computational aspects. *Computer Methods in Applied Mechanics and Engineering* 1987; **60**:153–173.
2. Lubliner J. A model of rubber viscoelasticity. *Mechanics Research Communications* 1985; **12**:93–99.
3. Le Tallec P, Rahier C, Kaiss A. Three-dimensional incompressible viscoelasticity in large strains: formulation and numerical approximation. *Computer Methods in Applied Mechanics and Engineering* 1993; **109**:233–258.
4. Le Tallec P. Numerical methods for nonlinear three-dimensional elasticity. In *Handbook of Numerical Analysis*, Ciarlet PG, Lions JL (eds), vol. 3. North-Holland: Amsterdam, 1994; 465–624.
5. Ciarlet PG. *Mathematical Elasticity*. North-Holland: Amsterdam, New York, 1988.
6. Holzapfel GA, Gasser TC. A viscoelastic model for fiber-reinforced composites at finite strains: continuum basis, computational aspects and applications. *Computer Methods in Applied Mechanics and Engineering* 2001; **190**:4379–4403.
7. Oden JT. *Finite Elements for Nonlinear Continua*. McGraw-Hill: New York, 1972.
8. Nocedal J, Wright SJ. *Numerical Optimization*. Springer Series in Operations Research. Springer: Berlin, 1999.
9. Miller K. Constitutive modelling of brain tissue: experiment and theory. *Journal of Biomechanics* 1997; **30**: 1115–1121.